

# Remote THz generation from two-color filamentation: long distance dependence

J.-F. Daigle,<sup>1,2,\*</sup> F. Théberge,<sup>3</sup> M. Henriksson,<sup>4</sup> T.-J. Wang,<sup>2</sup> S. Yuan,<sup>2</sup> M. Châteauneuf,<sup>3</sup>  
J. Dubois,<sup>3</sup> M. Piché,<sup>2</sup> and S. L. Chin<sup>2</sup>

<sup>1</sup>AEREX Avionique inc., Breakeyville, Québec, G0S 1E1, Canada

<sup>2</sup>Centre d'Optique, Photonique et Laser (COPL) & Département de Physique, de Génie Physique et d'Optique, Université Laval, Québec, G1V 0A6, Canada

<sup>3</sup>Defence R&D Canada-Valcartier, Québec, G3J 1X5, Canada

<sup>4</sup>FOI (Swedish Defence Research Agency), P.O. Box 1165, 581 11 Linköping, Sweden

\*[jean-francois.daigle.AEREX@drdc-rddc.gc.ca](mailto:jean-francois.daigle.AEREX@drdc-rddc.gc.ca)

**Abstract:** Remote terahertz (THz) generation from two-color filamentation is investigated as a function of the onset position of filaments. THz signals emitted by filaments produced at distances up to 55 m from the laser source were measured. However, from 9 m to 55 m, the THz signal decayed monotonically for increasing onset positions. With a simple calculation, the dominant factors associated to this decay were identified as group velocity mismatch of the two-color pulses and linear diffraction induced by focusing and propagating the second harmonic pulse.

©2012 Optical Society of America

**OCIS codes:** (190.4380) Nonlinear optics, four-wave mixing; (010.1300) Atmospheric propagation.

---

## References and links

1. M. Tonouchi, "Cutting-edge Terahertz technology," *Nat. Photonics* **1**(2), 97–105 (2007).
2. M. C. Kemp, C. Baker, and I. Gregory, "Stand-off explosives detection using terahertz technology," *Stand-off Detection of Suicide Bombers and Mobile Subjects*, pp. 151–165 (Springer, New York, 2006).
3. S. Nakajima, H. Hoshina, M. Yamashita, C. Otani, and N. Miyoshi, "Terahertz imaging diagnostics of cancer tissues with a chemometrics technique," *Appl. Phys. Lett.* **90**(4), 041102 (2007).
4. M. Lu, J. Shen, N. Li, Y. Zhang, C. Zhang, L. Liang, and X. Xu, "Detection and identification of illicit drugs using terahertz imaging," *Appl. Phys. (Berl.)* **100**, 103104 (2007).
5. A. Braun, G. Korn, X. Liu, D. Du, J. Squier, and G. Mourou, "Self-channeling of high-peak-power femtosecond laser pulses in air," *Opt. Lett.* **20**(1), 73–75 (1995).
6. A. Couairon and A. Mysyrowicz, "Femtosecond filamentation in transparent media," *Phys. Rep.* **441**(2-4), 47–189 (2007).
7. S.L. Chin, "Femtosecond laser filamentation," *Springer series on Atomic, Optical and Plasma physics*, LLC978–1-4419–0687–8 (Springer Science + Business media, New York, 2010).
8. V. P. Kandidov, S. A. Shlenov, and O. G. Kosareva, "Filamentation of high-power femtosecond laser radiation," *Quantum Electron.* **39**(3), 205–228 (2009).
9. H. Hamster, A. Sullivan, S. Gordon, W. White, and R. W. Falcone, "Subpicosecond, electromagnetic pulses from intense laser-plasma interaction," *Phys. Rev. Lett.* **71**(17), 2725–2728 (1993).
10. N. Karpowicz, X. Lu, and X.-C. Zhang, "Terahertz gas photonics," *J. Mod. Opt.* **56**(10), 1137–1150 (2009).
11. F. Théberge, W. Liu, P. T. Simard, A. Becker, and S. L. Chin, "Plasma density inside a femtosecond laser filament in air: strong dependence on external focusing," *Phys. Rev. E Stat. Nonlin. Soft Matter Phys.* **74**(3), 036406 (2006).
12. G. Méchain, C. D'Amico, Y.-B. André, S. Tzortzakis, M. Franco, B. Prade, A. Mysyrowicz, A. Couairon, E. Salmon, and R. Sauerbrey, "Range of plasma filaments created in air by a multi-terawatt femtosecond laser," *Opt. Commun.* **247**(1-3), 171–180 (2005).
13. J.-F. Daigle, Y. Kamali, M. Châteauneuf, G. Tremblay, F. Théberge, J. Dubois, G. Roy, and S. L. Chin, "Remote sensing with intense filaments enhanced by adaptive optics," *Appl. Phys. B* **97**(3), 701–713 (2009).
14. J. Kasparian, R. Sauerbrey, and S. L. Chin, "The critical laser intensity of self-guided light filaments in air," *Appl. Phys. B* **71**, 877–879 (2000).
15. A. Becker, A. D. Bandrauk, and S. L. Chin, "S-matrix analysis of non-resonant multiphoton ionisation of inner-valence electrons of the nitrogen molecule," *Chem. Phys. Lett.* **343**(3-4), 345–350 (2001).

16. C. D'Amico, A. Houard, M. Franco, B. Prade, A. Mysyrowicz, A. Couairon, and V. T. Tikhonchuk, "Conical forward THz emission from femtosecond-laser-beam filamentation in air," *Phys. Rev. Lett.* **98**(23), 235002 (2007).
17. Y. Chen, C. Marceau, W. Liu, Z.-D. Sun, Y. Zhang, F. Théberge, M. Châteauneuf, J. Dubois, and S. L. Chin, "Elliptically polarized terahertz emission in the forward direction of a femtosecond laser filament in air," *Appl. Phys. Lett.* **93**, 1116 (2008).
18. D. J. Cook and R. M. Hochstrasser, "Intense terahertz pulses by four-wave rectification in air," *Opt. Lett.* **25**(16), 1210–1212 (2000).
19. T.-J. Wang, J.-F. Daigle, S. Yuan, F. Théberge, M. Châteauneuf, J. Dubois, G. Roy, H. Zeng, and S. L. Chin, "Remote generation of high-energy terahertz pulses from two-color femtosecond laser filamentation in air," *Phys. Rev. A* **83**(5), 053801 (2011).
20. I. Babushkin, W. Kuehn, C. Köhler, S. Skupin, L. Bergé, K. Reimann, M. Woerner, J. Herrmann, and T. Elsaesser, "Ultrafast spatiotemporal dynamics of terahertz generation by ionizing two-color femtosecond pulses in gases," *Phys. Rev. Lett.* **105**(5), 053903 (2010).
21. W. Liu, F. Théberge, J.-F. Daigle, P. T. Simard, S. M. Sharifi, Y. Kamali, H. L. Xu, and S. L. Chin, "An efficient control of ultrashort laser filament location in air for the purpose of remote sensing," *Appl. Phys. B* **85**(1), 55–58 (2006).
22. N. Aközbek, A. Becker, and S. L. Chin, "Propagation and filamentation of femtosecond laser pulses in optical media," *Laser Phys.* **15**, 607–615 (2005).
23. C. Marceau, Y. Chen, F. Théberge, M. Châteauneuf, J. Dubois, and S. L. Chin, "Ultrafast birefringence induced by a femtosecond laser filament in gases," *Opt. Lett.* **34**(9), 1417–1419 (2009).
24. O. G. Kosareva, N. A. Panov, R. V. Volkov, V. A. Andreeva, A. V. Borodin, M. N. Esaulkov, Y. Chen, C. Marceau, V. A. Makarov, A. P. Shkurinov, A. B. Savel'ev, and S. L. Chin, "Analysis of dual frequency interaction in the filament with the purpose of efficiency control of THz pulse generation," *J. Infrared Milli Terahz Waves* **32**(10), 1157–1167 (2011).
25. Y. Liu, A. Houard, M. Durand, B. Prade, and A. Mysyrowicz, "Maker fringes in the Terahertz radiation produced by a 2-color laser field in air," *Opt. Express* **17**(14), 11480–11485 (2009).
26. S. A. Hosseini, Q. Luo, B. Ferland, W. Liu, S. L. Chin, O. G. Kosareva, N. A. Panov, N. Akozbek, and V. P. Kandidov, "Competition of multiple filaments during the propagation of intense femtosecond laser pulses," *Phys. Rev. A* **70**(3), 033802 (2004).
27. J. H. Marburger, "Self-focusing: theory," *Prog. Quantum Electron.* **4**, 35–110 (1975).
28. P. E. Ciddor, R. J. Hill, "Refractive index of air. 2. Group index," *Appl. Opt.* **38**(9), 1663–1667 (1999).
29. D. Strickland and G. Mourou, "Compression of amplified chirped optical pulses," *Opt. Commun.* **56**(3), 219–221 (1985).
30. J.-F. Daigle, A. Jaroń-Becker, S. Hosseini, T.-J. Wang, Y. Kamali, G. Roy, A. Becker, and S. L. Chin, "Intensity clamping measurement of laser filaments in air at 400 and 800 nm," *Phys. Rev. A* **82**(2), 023405 (2010).

## 1. Introduction

Due to recent achievements in laser sciences and technologies, terahertz (THz) generation and detection has attracted a lot of interest in multiple fields [1]. THz waves have strong material penetration [2] and specific absorption bands for identification of chemical products. These characteristics have motivated the recent development of THz 'tools' dedicated to environmental monitoring, medical sciences [3] and homeland security [4], that is now very active worldwide. However, because radiation in this spectral region is strongly absorbed and highly affected by linear diffraction during atmospheric propagation, it is still a hard task to deliver intense THz pulses at a remote position.

Laser filamentation [5–8] is currently one of the leading candidates that could potentially solve this problem. Experiments have shown that filaments could generate THz signals [9, 10] but also, that these filaments could be projected at any distance from the laser source ranging from centimetres [11] to several hundreds of metres [12, 13]. This promising behaviour could possibly circumvent the two issues mentioned above. With a simple modification of the effective focal length of a focusing telescope placed at the laser system output (see Fig. 1), this THz source could be arbitrarily positioned, close to the object to be illuminated.

Laser filaments result from a dynamic interplay between two nonlinear effects, namely Kerr self-focusing and defocusing from the self-induced plasma produced by multiphoton/tunnel ionization. This combination allows a propagation regime where the intensity is fixed over extended distances, much longer than the Rayleigh length. For a laser pulse at 800 nm, the Ti:Sapphire laser peak emission wavelength, the light intensity inside the

filament core is about  $50 \text{ TW/cm}^2$  [14] which is sufficiently high to induce high-order multiphoton processes such as 11-photon ionization of  $\text{N}_2$  [15].

Even though measurement of THz signals has been reported during single color filamentation (at 800 nm) [16, 17], the most promising scheme is probably the two-color technique [18] where the fundamental pulse co-propagates with its second harmonic (SH), at 400 nm, to produce a THz waves. A broadband THz pulse of  $2.8 \mu\text{J}$  was produced with this technique at a distance of 16 m from the focusing telescope [19].

It has been demonstrated, for point source plasmas, that the THz pulse is the result of a photocurrent induced by the asymmetric electric field distribution [20]. On the other hand, for elongated filaments, there is still no consensus whether the dominant mechanism is four-wave mixing from the two-color pulse or the photocurrent. In fact, because the conversion efficiency is highly dependent on the relative phase between the two co-propagating pulses, it is difficult to explain THz emission over such extended distances with the photocurrent model. Moreover, the plasma density inside the filament, required for the photocurrent, quickly decreases when generated at longer distance [11, 21]. However, this debate is beyond the scope of this paper and shall not be further discussed.

In this work, we put this remote THz source to the test by investigating how increasing the distance of filamentation onset, with the focusing telescope, impacts the produced THz signal. Using systematic measurements, the THz emission produced by laser filaments positioned at various distances from the laser source was characterized using a bolometer equipped with adequate filters. Even though the measured signal decayed monotonically as a function of distance, strong THz pulses were still observed when the filaments were positioned 55 m from the source, more than three times the longest distance previously reported. A simple numerical model was used to reproduce the observed behaviour and allowed the identification of the principal decaying factors involved.

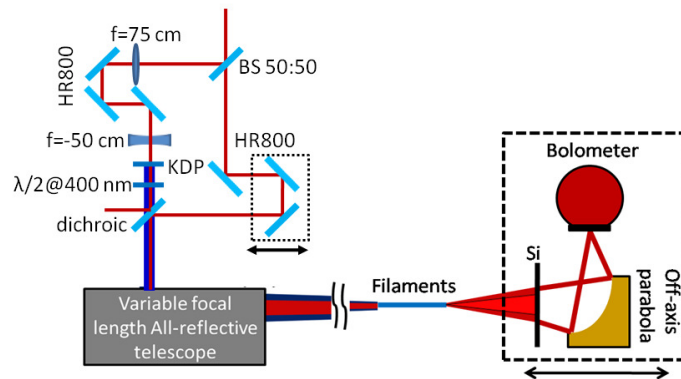


Fig. 1. Experimental setup for the generation and detection of THz pulses from two-color filamentation. 60 mJ transform limited pulses of 50 fs duration are directed to an interferometer. The first arm is used for second harmonic generation while the second is a delay line for adequate temporal superposition of the two pulses in the filament zone. The two pulses are recombined with a dichroic mirror and directed to an all-reflective telescope with a variable focusing length. The second harmonic pulse is focused together with the 800 nm to form filaments at the desired position. The produced THz pulses are measured with a helium-cooled bolometer protected with adequate filters. The off-axis parabola imaged the strong part of the filaments on the detector's surface.

## 2. Experimental scheme

The experiments were performed at Laval University where a 30 m long indoor horizontal path is available. Figure 1 presents a schematic view of the experimental setup. 60 mJ laser pulses of 50 fs transform limited duration at full width at half maximum were emitted at a 10 Hz repetition rate by a commercial Ti:Sapphire laser chain and directed to an interferometer.

A 50:50 beamsplitter divided the laser pulse in two parts. The reflected beam passed through a KDP crystal to produce a pulse at 400 nm (SH). A telescope composed of two lenses of focal lengths 75 cm and  $-50$  cm was used to control the divergence of the 400 nm pulses and ensure an optimal overlap of the two beams at the interaction zone. In the other arm, the transmitted fundamental pulse passed through a delay stage before it recombined with SH using a dichroic mirror. The energy in the transmitted beam was thus 30 mJ in the fundamental and  $\sim 1$  mJ in the SH. A half-wave plate at 400 nm was used to align the polarisations. The delay stage controlled the temporal overlap of the two pulses and was used to optimize every measurement.

The two co-propagating pulses passed through an all-reflective focusing telescope of variable focal length which was adjusted to produce filaments at the desired distance. The maximum propagation distance was increased to 60 m when a silver mirror was used at the end of the corridor to reflect both pulses. The aberrations introduced by the reflective-type focusing telescope were minimized by the telescope output mirror which consisted of an off-axis parabola.

The THz detection system was centered on the beam axis and positioned after the filaments. The signals were measured with a liquid helium-cooled bolometer whose sensitive surface was permanently protected by a polyethylene window that transmitted approximately 80% of the radiation above  $12\ \mu\text{m}$  ( $< 25$  THz). Behind this window, there was a movable filter consisting of a sapphire plate coated with zinc oxide and diamond layers which transmitted radiation above  $30\ \mu\text{m}$  ( $< 10$  THz). A 5 cm diameter off-axis parabola was used to image the strongest part of the filament onto the detector's sensitive surface. A silicon wafer, positioned before the parabola, blocked all the visible and near-infrared spectral components. Very weak THz signals were detected when SH was blocked. Therefore, a THz contribution resulting from the interaction of the strong post-filament core with the Si wafer was ruled out. For each filamentation distance, the position of the detection system with respect to the filaments was adjusted to optimize the measured signal. Moreover, we also measured the detected signals with other filters (e.g. fused silica ( $> 100$  THz), germanium ( $< 150$  THz), Teflon ( $< 5$  THz) and a quartz window covered with garnet ( $< 3.3$  THz)) to verify for contamination in the near and mid-infrared spectral regions and coarsely characterize the THz pulse spectral distribution. It was concluded that the measured radiation was almost entirely at frequencies smaller than 10 THz (see inset of Fig. 2). In addition, the measured THz spectrum remained almost constant as a function of the focal distance such that any effect of a frequency-dependent sensitivity of the bolometer would not affect the measurement.

The THz signal measured as a function of the filamentation distance is presented in Fig. 2 as red squares. The horizontal axis corresponds to the distance from the last optics in the focusing telescope to the strongest part of the filaments. Starting at 9 m, the signal received by the bolometer was rather strong. However, as the focusing distance was increased, the THz signal started to decrease rather slowly till the distance around 25 m. From here on, the signal suddenly shot down by more than one order of magnitude till 55 m. This distance was limited by the available space in the lab. The signal at this position was still about 9 times higher than the noise level.

Based on our knowledge of filamentation, such a steep signal decrease was not anticipated. In fact, experiments have shown that similar pulses projected at a remote position could efficiently produce filaments at 110 m and beyond [13]. Also, efficient THz generation due to the guiding [22, 23] of SH in the filament core was expected. Because the 800 nm pulse's peak power was fixed for all focal lengths, the number of filaments formed would not change significantly as the focal length increased; however, there would be a reduction of the plasma density as well as the clamped intensity [11]. The reduction of intensity inside the filaments with longer focusing would lead to a reduction of the THz signal. This tendency should continue along a certain experimental trend (slope) without break, in principle. The sudden break in the slope would mean that something else was happening. We explain this

sudden steep decrease of the THz signal as being due to the temporal walk-off between the 800 nm and 400 nm pulses in spite of the fact that the SH was guided (cross phase locking) in the filament core.

This is because the filament core is fed from the surrounding energy reservoir. The latter, being at a relatively low intensity is subject to a group index that is close to the linear value. The filament core simply follows the reservoir. The low intensity SH also propagates at a group velocity that is close to the value imposed by linear interaction with the medium. Thus, the walk-off between the pump and the SH does not depend upon the interaction between the two or guiding of the SH in the filament core via cross-phase-modulation. Consequently, any increase in filament length beyond this limit no longer contributes to the enhancement of the THz signal. The effect of this walk-off for THz generation during filamentation was described numerically for short focal lengths in [24].

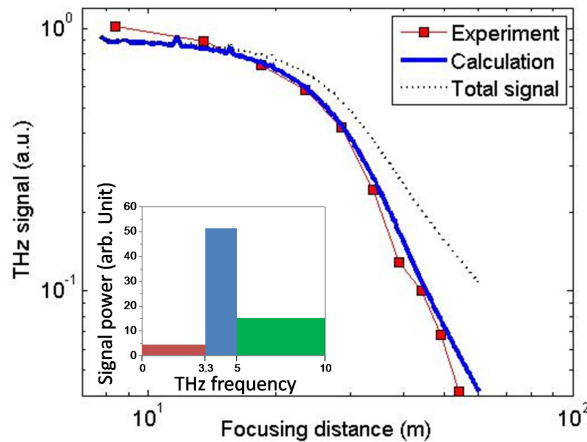


Fig. 2. THz signal measured as a function of the focusing distance and presented in a log-log scale. The horizontal axis corresponds to the distance between the telescope and the strongest part of the filaments. The dotted line corresponds to the total THz signal, independent of the parabola diameter, calculated for each focal position. Inset: Spectral distribution of the THz signal measured using different combinations of filters in front of the bolometer.

### 3. Modeling and discussion

In order to understand what the main causes for the signal decay with increasing focal length  $f$  were, the THz signals produced by the two-color pulses were simulated with a modified version of the model used in [25]. Even though this model contained important approximations, it could reproduce very well the experimental data obtained. The purpose of this calculation is to demonstrate that the dominant factors leading to the observed reduction of the signal are not related to any nonlinear properties of the filaments or the THz generation mechanism. In fact, most of the equations used in this model assume multiple approximations that would normally be unavoidable in most filamentation modeling. Among those approximations we have neglected multi-filamentation competition [26], focal length-dependent filament properties (plasma density, intensity, number of filaments etc.) and self-focusing of the SH pulses. These approximations were made to emphasize the fact that the dominant mechanisms leading to the observed behaviour are not related to a modification of the filaments' properties when formed at long distance. Instead, more basic and fundamental optical phenomena such as linear diffraction and group velocity mismatch can explain the observations.

A four-wave mixing model for THz emission originating from the interaction of a single, cylinder-like filament of finite length and fixed intensity with a focused SH Gaussian pulse,

whose focal waist is much larger than the filament diameter, was used as approximation of our experiment. Because the 800 nm pulse had a fixed peak power, the number of filaments produced is nearly constant and they would ‘crowd’ around the focal region each with essentially a constant intensity inside because of intensity clamping. We approximate this bundle of filament as an effective single filament. The modeling conditions are presented in Fig. 3 where a 800 nm pulse, focused to form a filament of length  $L_{fil}$ , is superposed to a focused Gaussian pulse at 400 nm. A screen, positioned at a distance  $d$  from the filament end, represents the collecting parabola used to collect the signal onto the detector. When the focusing position  $f$  moves further away, the filament length becomes longer and, therefore, the amount of THz signal produced during the interaction should have increased. In fact, the filament length can, roughly speaking, be approximated as  $L_{fil} = f(1 - z_f / (z_f + f))$  where  $z_f$ , the self-focusing distance, depends on the initial beam diameter and the pulse power [27]. This definition of  $L_{fil}$  implies that the filament always ends at the telescope focal position, which was the case in our experiment. Because it is rather hard to evaluate for real world beams whose transverse intensity profiles are not Gaussian,  $z_f$  was left as a fitting parameter and ultimately fixed to  $z_f = 180$  m. Using Marburger's formula [27], which determines the self-focusing distance  $z_f$  as a function of the pulse peak power,  $z_f = 180$  m can be achieved in air with 0.6 TW laser pulses of 2.5 cm transverse radius. Interestingly, in our experiment, the peak power of the 800 nm pulses was also 0.6 TW. In addition to reflecting the high quality of this laser beam line, this result further supports the data obtained by this model.

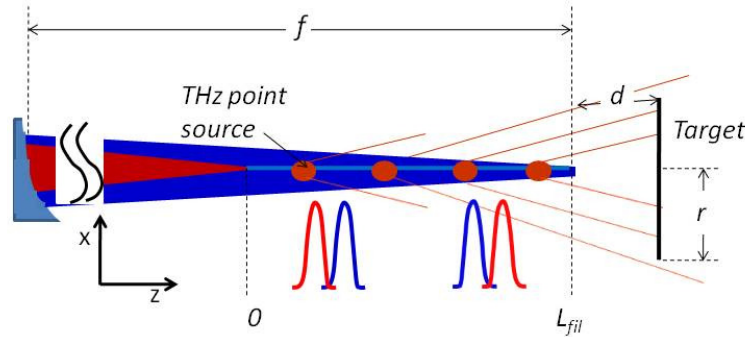


Fig. 3. Schematic representation of the numerical model developed.

Both pulses were considered perfectly Gaussian in the temporal domain. SH was assumed Gaussian in the transverse plane and even though its peak power was higher than the critical power, self-focusing was neglected. If we suppose that this filament consists of a series of THz point sources aligned along the propagation axis  $z$  and that the polarisation of both pulses is linear and parallel, the THz signal emitted by each point source is then given by:

$$E_{THz}(z, f) = \frac{E_{\omega}^2 E_{2\omega}}{z_{R,2\omega}(f) \sqrt{1 + \left(\frac{z - L_{fil}}{z_{R,2\omega}}\right)^2}} e^{-\left(\frac{\theta(z, f)}{\tau}\right)^2} e^{-i\phi(z, f)}. \quad (1)$$

In this equation,  $z=0$  corresponds to the onset position of the filaments,  $E_{\omega}$  and  $E_{2\omega} D_{2\omega} / z_{R,2\omega}(f)$  correspond to the pulses peak electric field measured at the focal position for the fundamental and SH pulses respectively,  $\tau$  is the pulse duration measured at  $e^{-1}$ ,  $z_{R,2\omega}(f)$  is the calculated Rayleigh range for the focused second harmonic pulse and  $D_{2\omega}$  is SH initial beam diameter.  $\theta(z, f)$ , which describes the temporal overlap of the two pulses at a position  $z$  and  $\phi(z, f)$ , which corresponds to the generated THz pulse phase are given by:

$$\theta(z, f) = \frac{2}{c} \left( z - \frac{L_{fil}}{2} \right) (n_{g,\omega} - n_{g,2\omega}) \quad (2)$$

$$\varphi(z, f) = \left( \omega_{THz} n_{g,\omega} - 2\omega_F n_{\omega} + \omega_{SH} n_{2\omega} \right) \frac{z}{c} + \tan^{-1} \left( \frac{z - L_{fil}}{z_{R,2\omega}(f)} \right) - 2 \tan^{-1} \left( \frac{z - L_{fil}}{z_{R,\omega}(f)} \right) \quad (3)$$

In Eq. (2), the  $n_{g,i}$ 's correspond to the group velocity refractive indices of both pulses in normal atmosphere and  $c$  is the speed of light. On the other hand, Eq. (3) is the THz pulse phase where the  $n_i$ 's are the refractive indices of air of the pump pulses,  $\omega_{THz}$  is the angular frequency of the THz pulse produced and  $\omega_F$  and  $\omega_{SH}$  correspond to the angular frequencies present within the broadband pump pulses required to produce  $\omega_{THz}$ . The two terms with the arctangent account for the Gouy phase shift of each beam that occurs at the waist but since the interaction zone (filament) ends at the focus, its effect is rather small. The first term describes the group velocity mismatch between the fundamental and the SH pulse. The refractive indices modifications induced by self-focusing and the presence of plasma were neglected. The values of  $n_{g,i}$  were obtained from the model developed in [28]. This assumption is valid because, even though both pulses interact in the filament core (guiding of SH and cross phase modulation), it is the energy reservoir, which is at a much lower intensity, that imposes the pulse propagation speed. The filament core only follows the peak intensity of the pump pulse. In addition, if the nonlinear contributions to the index of refraction were to be included in the model, the difference in group velocities would be increased leading to a more important walk-off between the two pulses. In fact, because the reservoir of the fundamental pulse is much more intense than SH, the refractive index contribution from cross phase modulation is larger for SH such that its group velocity decreases more than that of the fundamental pulse. Once again, because the properties of air are not well known in the THz spectral range, approximations were made in Eq. (3). In fact, the refractive index of air at THz frequencies was assumed equal to unity and the THz pulse traveled at the speed  $c$ . All these assumptions were made to keep the focus on the main causes of the signal decay for long focal lengths.

As a result, for filaments formed with a focal length  $f$ , the total THz field reaching a target of transverse coordinate  $x$  positioned at a distance  $d$  from the end of the filament is given by:

$$E_{THz}(x) = \int_0^{L_{fil}} \frac{E_{THz}(z)}{\sqrt{(L_{fil} + d - z)^2 + x^2}} e^{-i \left( \frac{\omega_{THz}}{c} \sqrt{(L_{fil} + d - z)^2 + x^2} \right)} dz. \quad (4)$$

Finally, the total THz power collected by the parabola of radius  $r$  is obtained from:

$$P_{THz} = \pi c \varepsilon \int_0^r E_{THz}^*(x) E_{THz}(x) x dx. \quad (5)$$

The calculation was performed for ten different THz frequencies between 0.1 to 10 THz and the output data, shown as a blue line in Fig. 2, corresponds to the sum of the all these components corrected based on the spectral measurements shown in Fig. 2. In this simulation,  $E_{\omega} = 1$ ,  $E_{2\omega} = 1/30$ ,  $\tau = 75$  fs for both pulses (at  $e^{-1}$ ),  $d = 50$  cm and  $r = 2.5$  cm correspond to the radius of the collecting parabola. Good agreement was obtained and that even if multiple effects were neglected. This shows that the dominant factors resulting to this decay are not related to the filaments' properties.

In the experiment, the limited diameter parabola only captured a fraction of the total THz signal produced by the filaments, especially for long focal lengths of the telescope. In order to verify if this could have lead to the formation of the knee at 25 m, the calculation was repeated by considering a 10 m diameter parabola. The result is shown in Fig. 2 as a dotted line. It shows, apart from a change in the slopes at long distances, a very similar trend

including the inflection around 25 m. Therefore, the sudden slope change observed is not related to a reduced collection efficiency attributed to a limited diameter parabola.

The first reason why the signal decreased with increasing  $f$  is destructive interference of the multiple THz sources aligned along the filament, and this is independent of the physical process producing the THz waves, i.e. the photocurrent or the four-wave mixing. Indeed, the electromagnetic wavefronts emitted by the THz point sources interfere as they travel towards the parabola. Elongating the filament increases the probability of finding two point sources whose electromagnetic fields cancel at the parabola. As a result, destructive interference decreases the on-axis intensity which produces a rather divergent THz beam. Since most of the THz energy propagates at an angle with respect to the propagation axis, this effect further deteriorates the collection efficiency because, beyond a certain filament length, the limited radius parabola can no longer capture all the produced THz radiation.

Another important factor is related to the diffraction that the SH pulse encounters when it is focused and propagates extended distances. During the experiment, even though self-focusing could have been significant, no filamentation of SH was observed. Under these circumstances, SH was affected by diffraction and the focal spot diameter of the SH pulse increased linearly with increasing  $f$ . Based on the Rayleigh criterion, the focal intensity of SH should behave as

$$I = \frac{\pi P D_{2\omega}^2}{4\lambda_{2\omega}^2 f^2} = \frac{P}{\pi z_{R,2\omega}^2}. \quad (6)$$

This equation, where  $P$  is the pulse peak power,  $D_{2\omega}$  is its initial diameter and  $\lambda_{2\omega}$  the central wavelength, shows that  $I$  is inversely proportional to the square of the focusing distance. In the model, since the THz intensity produced by the filament is proportional to the intensity of the SH pulse, increasing the focal length to  $f + \Delta f$  will intrinsically reduce the

THz intensity by a factor that is proportional to  $\left(\frac{f}{f + \Delta f}\right)^{-2}$ . In fact, the calculated total signal decreases with a slope of  $-2$  beyond 25 m.

As of now, it seems that increasing the focal length or increasing the f-number in order to generate the filaments further away can only impact negatively on the THz signal captured by the detector. However, as mentioned earlier, increasing  $f$  produces a longer filament, thus, a longer interaction zone and ultimately, we should expect stronger THz signals. When  $f < z_f$ , the filament length will grow as  $f^2$ , with reduced growth rate as the two distances become more equal. This resulted in a reduced decaying slope which was measured to be  $-0.9$  for the THz signal in Fig. 2, for focal lengths shorter than 20 m. This decay was mainly due to the decrease of the SH intensity and the lower collection efficiency for longer distance. However, the THz generation has another limitation, attributed to group velocity mismatch of the two pulses, which imposes a maximal length they can be superposed while propagating in air. In fact, even though self-group phase locking [22] of the two pulses and guiding [23] of the SH pulse could have occurred in the filament core, the surrounding energy reservoir still propagates in a quasi-linear way at a group velocity which depends on the pulse's wavelength. Thus group velocity mismatch of two pulses should occur during filamentation in air. When it comes to femtosecond pulses, this limit can appear at short propagation distances. In fact, the walk-off length (*WOL*) of two pulses at different wavelengths propagating in air is defined as

$$WOL = \left| \frac{2\tau c^2}{v_{g,\omega} - v_{g,2\omega}} \right| \quad (7)$$

where  $v_g$  correspond to the group velocities of each pulses in air. Assuming that both the fundamental and SH pulses had a pulse duration of 75 fs, the maximum interaction length was limited to  $WOL = 1.8$  m such that any section of a filament whose length exceeded *WOL*

would not produce significant THz. The slow decay before 25 m and the knee observed in Fig. 2 both for the experiment and the calculation is a direct consequence of this limitation. In fact, in our model, filaments longer than 1.8 m were obtained for focal lengths ranging between 18 m and 25 m. The interaction length then becomes constant for longer focal distance, and the signal started to decrease at a faster rate resulting in a slope change in the log-log plot.

The results presented show the difficulties that we have to face when it comes to produce strong THz pulses beyond 100 m from the source with the current method and laser. We however decided to look at the stated problems as new challenges to overcome and, would like to propose possible avenues other than the usually suggested solutions. Among those intuitive propositions we have increasing the initial beam size to reduce the f-number or increasing the SH pulse intensity. Another possible path consists in finding a method to increase *WOL*. Based on Eq. (7), this could easily be done by increasing the pulse duration. However this method should be used with care because, in current CPA systems [29], increasing the pulse duration is often realized through chirping the pulse at the expense of pulse peak power. This could rapidly result in a reduction of the filaments' length and robustness.

Because the difference in group refractive index between the fundamental and SH pulses becomes less important, increasing the fundamental pulse wavelength also leads to an elongation of *WOL*. With a quick estimation using Eq. (7) and the group velocities  $v_g$  obtained from the model presented in [27], the total THz signal could be increased by a factor 5 if the fundamental wavelength was shifted from 800 nm to 1.7  $\mu\text{m}$ . However, this technique also has a drawback. In fact, as expressed in Eq. (6), the focal intensity is inversely proportional to the square of the wavelength. Therefore, this focal intensity diminution of SH reduces the 500% enhancement, obtained from the elongated *WOL*, to a mere 11%.

Even though remote generation of powerful THz is challenging, we still believe that increasing the wavelength and the pulse width of the fundamental pulse could lead to a significant enhancement of the THz signal produced during two-color filamentation at long distance. In fact, because an increasing number of photons are required to ionize atmospheric molecules at longer pump wavelength, the formation of a stabilized filament could occur at a clamped intensity which increases with the fundamental wavelength. Assuming that four-wave mixing is the dominant mechanism for extended filaments, the THz signal would be proportional to the square of the filament's clamped intensity. In fact, in this scenario, two photons of the fundamental pulse are required to produce a single THz photon. However, because there are very few laser sources available worldwide sufficiently powerful to induce filamentation in air at wavelengths longer than 800 nm, both of these hypotheses have not yet been verified experimentally. Previous measurements revealed that the clamped intensity inside filaments increased by a factor 2.5 when the pulse peak wavelength was changed from 400 nm to 800 nm [30].

#### 4. Conclusions

In this work, remote THz generation from two-color filamentation in air was put to a test and strong THz signals were still observed when the filaments were positioned 55 m from the source, more than three times the longest distance previously reported. The results obtained revealed that as the filament bunch moved towards longer distances, the produced THz signal decreased monotonically. A simple numerical model revealed that the dominant factors related to this decay are not related to the filaments' properties. The decaying mechanisms were rather identified as group velocity mismatch between the two-color pulses and, diffraction caused by the long propagation of the SH pulse.

The conclusions drawn from this study show that the production of strong THz pulses beyond 100 m from the current laser source are very challenging. However, two possible scenarios were proposed to improve the technique. The most promising method consists in

increasing the clamped intensity by using a laser pulse with a longer wavelength. Laser sources that could put this idea to a test start to emerge; perhaps someone will perform the experiment shortly?

### **Acknowledgments**

We acknowledge the support from the Natural Sciences and Engineering Research Council, a Defence Research & Development Canada Applied Research Program, the Canadian Institute for Photonic Innovation, the Canadian Foundation for Innovation, Fonds Québécois de Recherche pour la Nature et la Technologie, and the Canadian Research Chair. M. Henriksson acknowledges strategic research funding from the Swedish Armed Forces. The authors acknowledge technical support from Michèle Cardinal, Marcellin Jean, Alain Fernet and Mario Martin.